Compensation of interchannel nonlinearities using enhanced coupled equations for digital backward propagation

Eduardo F. Mateo* and Guifang Li

CREOL, The College of Optics and Photonics, University of Central Florida, 4000 Central Florida Boulevard, Orlando, Florida 32816, USA

*Corresponding author: emateo@creol.ucf.edu

Received 29 January 2009; revised 29 March 2009; accepted 7 April 2009; posted 9 April 2009 (Doc. ID 106893); published 28 April 2009

Enhanced coupled-nonlinear equations are introduced for full compensation of cross-phase modulation and partial compensation of four-wave mixing (FWM) via split-step digital backward propagation. Compared to full FWM compensation, the new backward propagation equations provide a significant reduction in the number of steps required in the split-step method. This increased step size together with more relaxed sampling requirements reduced the computational load by more than a factor of 20. © 2009 Optical Society of America

OCIS codes: 060.1660, 060.4370.

1. Introduction

In long-haul fiber transmission systems, fiber chromatic dispersion, Kerr nonlinearity, and amplifier noise are responsible for signal degradation, limiting the transmission capacity. Recently, electronic precompensation and/or postcompensation of transmission impairments have attracted significant attention due to the fast development of coherent detection and digital signal processing (DSP), which constitute the enabling technologies for electronic impairment compensation [1,2]. Among all the transmission impairments, interchannel nonlinearities play a major role in limiting the performance of wavelength division multiplexing (WDM) systems. Impairment postcompensation can be electronically implemented by reversing the linear and nonlinear distortions experienced through fiber transmission [2]. In order to do so, the optical field is backward propagated by implementing, in the digital domain, the numerical method for solving the backward propagation equations. One of the fundamental challenges in the DSP implementation of backward propagation is the reduction of the computational load. In this paper, a system of enhanced coupled (EC) nonlinear Schrödinger equations (NLSEs) is proposed to fully compensate for cross-phase modulation (XPM) and partially compensate for four-wave mixing (FWM). A 24×100 Gbit/s 16-QAM WDM system has been simulated, where postcompensation using EC-NLSEs is compared with full XPM + FWM compensation using the total field NLSE. Transmission performance and computation efficiency are analyzed in both cases.

2. XPM and FWM Postcompensation using Backward Propagation

In a coherently detected system, a full reconstruction of the optical field can be achieved by beating the received field with a co-polarized local oscillator. The reconstructed field will be used as the input for backward propagation in order to compensate for the transmission impairments. Let $\hat{E}_m$ be the field envelope of the mth received channel, where $m = \{1, 2, , N\}$ and N is the total number of channels. The reconstructed total optical field is given by

0003-6935/09/2500F6-05$15.00/0

$$E = \sum_{m=1}^{N} \hat{E}_m \exp(im\Delta\omega t), \tag{1}$$

where $\Delta f = \Delta\omega/2\pi$ is the channel spacing. The total-field backward propagation equation (T-NLSE) is given by [3]

$$-\frac{\partial E}{\partial z} + \frac{\alpha}{2}E + \frac{i\beta_2}{2}\frac{\partial^2 E}{\partial t^2} - \frac{\beta_3}{6}\frac{\partial^3 E}{\partial t^3} + i\gamma|E|^2 E = 0, \tag{2}$$

where β_j represents the jth-order dispersion, α is the absorption coefficient, γ is the nonlinear parameter, and t is the retarded time frame. Equation (2) governs the backward propagation of the total field including second- and third-order dispersion compensation and the full compensation of self-phase modulation (SPM), XPM, and FWM.

Alternatively, the effect of FWM can be omitted in backward propagation by introducing the field expression in Eq. (1) into Eq. (2), expanding the nonlinear term, and neglecting the so-called FWM terms, that is [3,4],

$$\begin{aligned} &-\frac{\partial \hat{E}_m}{\partial z} + \frac{\alpha}{2}\hat{E}_m + \sum_{p=1}^{3} K_{pm}\frac{\partial^p \hat{E}_m}{\partial t^p} \\ &+ i\gamma\left(2\sum_{q=1}^{N}|\hat{E}_q|^2 - |\hat{E}_m|^2\right)\hat{E}_m \\ &= 0, \end{aligned} \tag{3}$$

where p is the derivative order and the coefficients K_{pm} are given by

$$\begin{aligned} K_{1m} &= m\beta_2\Delta\omega - \frac{1}{2}m^2\beta_3\Delta\omega^2, \\ K_{2m} &= \frac{1}{2}i\beta_2 - \frac{1}{2}m\beta_3\Delta\omega, \qquad K_{3m} = -\frac{1}{6}\beta_3. \end{aligned} \tag{4}$$

The system of coupled equations (C-NLSEs), given by Eq. (3), describes the backward evolution of the baseband WDM channels where dispersion, SPM, and XPM are compensated.

Equations (2) and (3) are solved in the digital domain by the well-known split-step Fourier method (SSFM) [3]. From the computational perspective, two fundamental parameters have to be considered when assessing the computation requirements for T-NLSE/C-NLSEs approaches. These parameters are the sampling rate and the SSFM step size. For postcompensation using T-NLSE, each detected channel has to be upsampled so that the bandwidth of the reconstructed full-optical field is wide enough to avoid aliasing of newly generated FWM products. This constraint is made explicit by the following relation for the sampling rate:

$$S_{\text{T-NLSE}} = 2\frac{N\Delta f}{B}, \qquad \text{samples/symbol}, \tag{5}$$

where B the symbol rate per channel. The above formula forces the sampled bandwidth to be twice the optical WDM bandwidth. Alternatively, XPM compensation using C-NLSEs does not create new frequency components. Hence, an accurate backward propagation can be performed under the Nyquist limit, i.e., using 2 samples per symbol. Together with the sampling rate, the SSFM step size is of utmost importance when computational efficiency is considered. In [4], a detailed analysis of the step size requirements for both XPM and XPM + FWM compensation is performed, showing that correct FWM postcompensation requires remarkably smaller step sizes compared to XPM compensation, which translates into a higher computational load.

3. Enhanced Coupled Equations and Partial FWM Compensation

Due to the step size and sampling requirements, FWM compensation requires a large amount of calculation compared to XPM compensation only. However, for low dispersion regimes, FWM can substantially impair the signal due to an increased degree of phase matching. In this paper, we propose a method for the partial compensation of FWM using an enhanced system of coupled equations, where FWM interaction is compensated on a channel-by-channel basis, by considering the nonlinear mixing of the neighboring channels. In this vein, Eq. (3) can now be rewritten as

$$\begin{aligned} &-\frac{\partial \hat{E}_m}{\partial z} + \frac{\alpha}{2}\hat{E}_m + \sum_{p=1}^{3} K_{pm}\frac{\partial^p \hat{E}_m}{\partial t^p} \\ &+ i\gamma\left(2\sum_{q=1}^{N}|\hat{E}_q|^2 - |\hat{E}_m|^2\right)\hat{E}_m + F_{2m} + F_{4m} \\ &= 0, \end{aligned} \tag{6}$$

where

$$F_{2m} = 2\hat{E}_{m+1}\hat{E}_{m-1}\hat{E}_m^*, \tag{7}$$

$$\begin{aligned} F_{4m} = {} & \hat{E}_{m+1}^2\hat{E}_{m+2}^* + \hat{E}_{m-1}^2\hat{E}_{m-2}^* + 2\hat{E}_{m-1}\hat{E}_{m+1}\hat{E}_{m+1}^* \\ & + 2\hat{E}_{m+1}\hat{E}_{m-2}\hat{E}_{m-1}^* + 2\hat{E}_{m+2}\hat{E}_{m-2}\hat{E}_m^*. \end{aligned} \tag{8}$$

The above system of equations, Eq. (6), will be referred to as enhanced coupled equations (EC-NLSEs), where F_2 represents the FWM interaction of two neighboring channels and F_4 includes the interaction of four neighboring channels. Although only a small number of FWM terms are considered in Eq. (6), these terms are highly phase matched and improved results are expected without significant increase of computational load (note that in the SSFM the dispersive term requires the highest computational load). The SSFM implementation of

Eq. (6) is done in a perturbative manner, where the nonlinear operator (see for example [3,4]) for the jth step is approximated by

$$\hat{E}_m^{j+1} = \hat{E}_m^j \exp(i\gamma|\hat{E}_m^j|^2 h) + h(F_{2m}^j + F_{4m}^j). \quad (9)$$

Figure 1 depicts a block diagram of the SSFM step for the EC-NLSEs. The diagram represents the implementation of the jth step for the asymmetric SSFM [3] including the perturbative FWM terms, where $P(x) = |x|^2$, $E(x) = \exp(i\gamma hx + h\alpha/2)$, $D_m(x) = \mathcal{F}^{-1}[H_m \mathcal{F}(x)]$, and

$$H_m(\omega) = \exp\left[\left(i\beta_2 \frac{(\omega - m\Delta\omega)^2}{2} + i\beta_3 \frac{(\omega - m\Delta\omega)^3}{6}\right)h\right]. \quad (10)$$

Equation (9) is valid provided that the FWM contribution to the fields evolution is slow within the SSFM step. In general and for WDM systems, the SSFM step size is limited by dispersive effects. In [4], it is shown that the step size for XPM compensation is limited by the walk-off length, whereas the dispersive phase mismatch limits the step size for FWM compensation. In this context, it is shown that FWM phase-mismatch length scales with the inverse square of the total optical bandwidth whereas the walk-off length scales with inverse of the total optical bandwidth. For a large number of channels, FWM requires a much smaller step size to be able to follow the changes of the optical field induced by the nonlinear mixing of the fields. In the EC-NLSEs case, only FWM between neighboring channels is considered. Therefore, the effective optical bandwidth is drastically reduced as well as the degree of phase mismatch, which yields a larger phase-mismatch length. As a consequence, if the number of neighboring channels is a small fraction of the number of WDM channels interacting through XPM, the phase-mismatch length becomes larger than the walk-off length. This ensures that the field variations due to XPM are faster than the variations due to FWM allowing the perturbative expression given by Eq. (9).

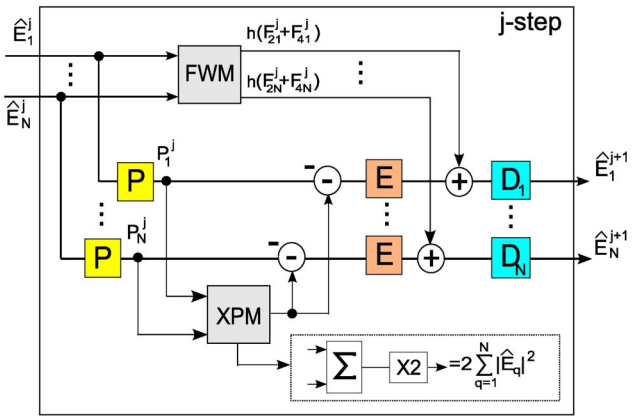

Fig. 1. (Color online) Block diagram of the SSFM step implementing the EC-NLSEs.

4. Simulation Results and Discussion

Figure 2 depicts the simulated transmission system showing the postprocessing stages for the different compensation schemes. A 24-channel 16-QAM WDM system modulated at a bit rate of 100 Gbits/s has been simulated in a fiber link consisting of 10 spans of 100 km/span. The optical fiber has the following parameters: dispersion parameter $D = 2$ ps/km/nm, dispersion slope $D_s = 0.045$ ps/km/nm^2, loss $\alpha = 0.2$ dB/km, and nonlinear coefficient $\gamma = 1.46$ /W/km. A noise figure of 5 dB is considered for the erbium-doped fiber amplifiers.

After transmission and coherent detection, the baseband complex envelopes are obtained from the in-phase and quadrature outputs of an optical hybrid (more details of the coherent receiver can be found in [2]). For XPM + FWM compensation using T-NLSE, the channels are upsampled and upconverted to its corresponding frequency band. Subsequently, the channels are combined and backward propagated using Eq. (2). Finally, electronic demultiplexing is performed. In the (C, EC)-NLSEs cases, backward propagation is performed directly using the channels at baseband. Hence, upconversion, upsampling, and demultiplexing are not required. As shown in Fig. 2, a set of local oscillators (LOs) is used for coherent detection and reconstruction of each WDM channel. Since FWM is a phase-sensitive process, the relative phase of the WDM channels has to be known for any backward propagation scheme that involves total or partial FWM compensation. From a hardware point

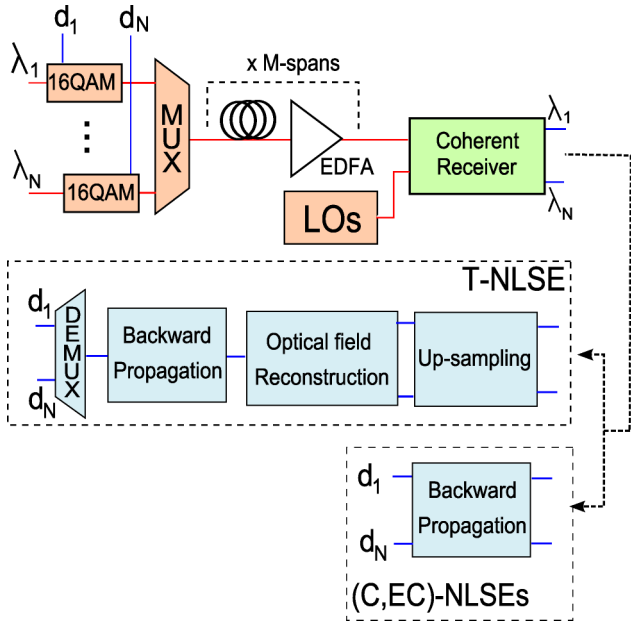

Fig. 2. (Color online) Scheme of the WDM transmission and digital postprocessing stages for backward propagation implementation using T-NLSE and (C, EC)-NLSEs. MUX, multiplexer; DEMUX, demultiplexer.

of view, and as discussed in [2], the phases of the LOs have to be locked to preserve the relative phase of the reconstructed WDM channels after coherent detection. A set of phase-locked LOs can be created by techniques used for frequency comb generation (see, for example, [1]). In addition, phase tracking among the recovered optical fields of these WDM channels is needed.

Figure 3 shows simulation results comparing T-NLSE, EC-NLSEs, and C-NLSE for backward propagation. In terms of performance, it is shown that postcompensation of interchannel nonlinearities substantially increases the performance with respect to dispersion compensation only. Additionally, full FWM compensation increases the maximum Q value by around 2 dB with respect to XPM compensation only (C-NLSEs). This difference can be reduced using the EC-NLSEs system, where at least four neighboring channels have to be included to achieve substantial improvement. In Fig. 4, the Q value of the WDM channels is shown for each postcompensation case. For the C-NLSEs case, it is observed that the penalty increases for the central channels due to a higher density of newly generated FWM products [5]. However, including five-channel FWM interaction through EC-NLSEs, FWM is partially compensated, improving the overall performance. Figure 5 shows the Q value versus the step size where vertical lines indicate the optimum step size for each case, i.e., $h_{\text{T-NLSE}} = 167\,\text{m}$ and $h_{\text{(C,EC)-NLSE}} = 2\,\text{km}$. As expected, due to the reduced bandwidth of the FWM interaction, the EC-NLSEs system does not require a reduced step size, which remains limited by the walk-off length.

In order to quantify computation requirements, the following figure of merit can be defined, $C = n_{\text{eq}} \times S/h$, where n_{eq} is the number of backward equations to be solved, S is the sampling rate, and h is the step size. According to the sampling requirements (previously introduced) and the required step sizes, the following values are obtained for each postcompensation case, i.e., $C_{\text{T-NLSE}} = 575\,\text{samples/symbol/km}$, $C_{\text{(C,E)-NLSE}} = 24\,\text{samples/symbol/km}$. Clearly, full FWM compensation using T-NLSE requires an extraordinary amount of computation resources compared to EC-NLSEs, which requires ~24 times fewer calculations. In addition to the computational cost, the parallel character of the (C, EC)-NLSEs cases may have an important impact in the DSP implementation, giving rise to a remarkable decrease in the system latency.

We have seen that together with the SSFM step size, the sampling requirements for FWM play a fundamental role in the computation efficiency for backward propagation. To quantify the role of the sampling rate in the system performance, Fig. 6 shows the Q values per channel, for the T-NLSE compensation scheme, at two different sampling rates, i.e., higher and lower than the theoretical limit given

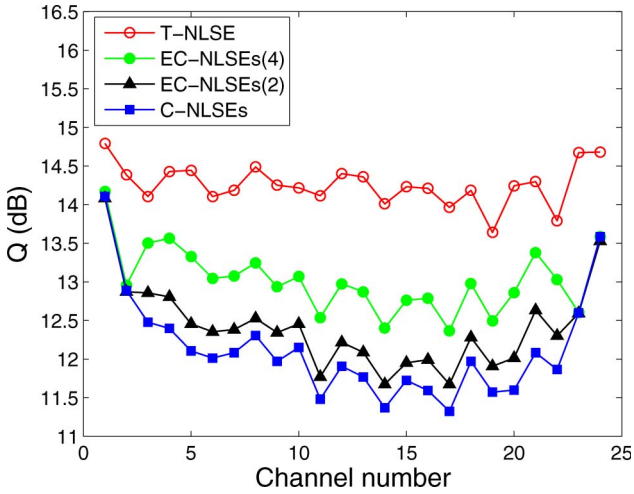

Fig. 4. (Color online) Distribution of Q values with WDM channels (power/channel = 0.2 dBm).

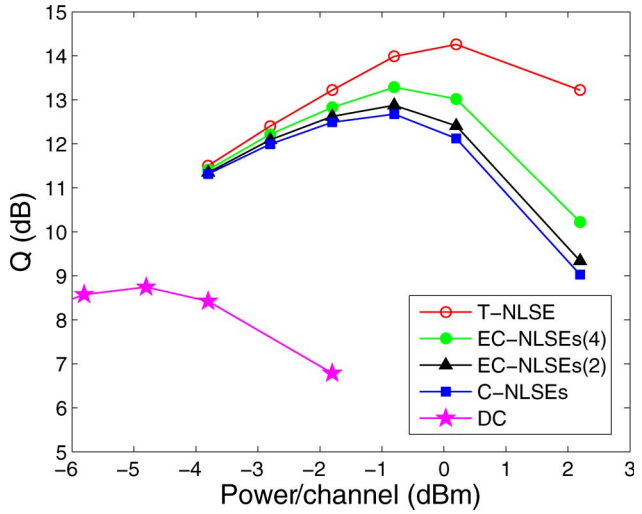

Fig. 3. (Color online) Performance versus power for the different postcompensation cases, where EC-NLSEs(2, 4) represents the EC-NLSEs with (2, 4) neighboring channels (the Q value is averaged over all the WDM channels). Additionally, results for dispersion compensation (DC) only are shown.

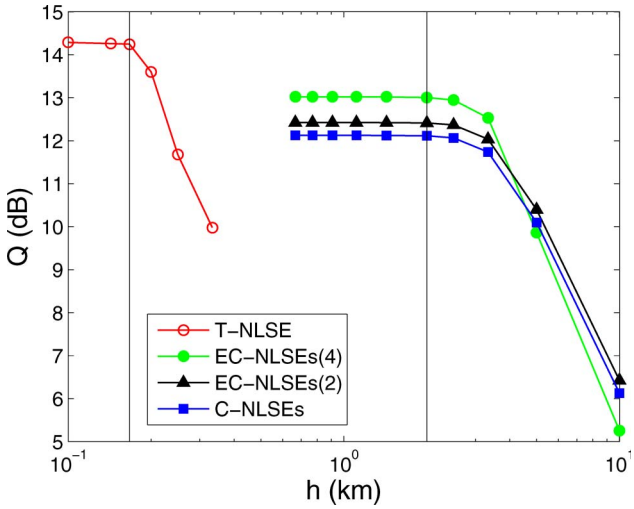

Fig. 5. (Color online) Averaged Q value as a function of the SSFM step size for the respective optimum powers.

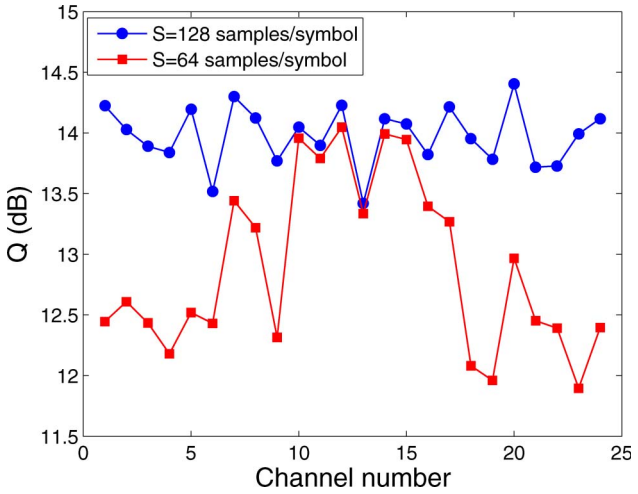

Fig. 6. (Color online) Q value per channel for different upsampling factors (power/channel = 0.2 dBm).

by Eq. (5), i.e., $S_{\text{T-NLSE}} = 96$ samples/symbol. It is shown that, at a low sampling rate, the edge channels are distorted due to errors in the estimation of FWM products. During transmission in the physical domain, FWM products are created outside the WDM channels. These products are usually small, inducing a negligible channel distortion. Although these newly generated waves can be coherently detected and backward propagated together with the WDM channels, simulations demonstrated that its contribution does not improve the performance in a significant way. Similarly, digital backward propagation creates FWM outside the WDM band. In this case, an insufficient sampling will create aliasing, making the FWM products to fall into the WDM channels. These aliased FWM products are mixed with the channels and propagated under a different phase-matching condition. This artificially increases the FWM efficiency and induces channel distortion. In contrast, when the sampling rate is increased, i.e., $S > S_{\text{T-NLSE}}$, aliasing is prevented. Here, the newly generated waves, now located outside the WDM band, propagate under realistic phase-matching conditions, which prevents any artificially induced FWM enhancement. Therefore, as in the physical domain, the WDM channels are not distorted by *out-of-band* products, as is shown in Fig. 6 for $S = 128$ samples/symbol.

5. Conclusion

A set of enhanced coupled NLSEs has been used for full postcompensation of interchannel XPM together with partial compensation of FWM. Simulation results show that FWM can be partially compensated with a negligible increase on the computational load with respect to XPM compensation only. The results have been compared with full XPM+FWM compensation using the total-field NLSE, showing that postcompensation using EC-NLSEs incurs a Q-value penalty of 1 dB due to the partial compensation of FWM. However, by considering both sampling and step size requirements of the split-step Fourier method, postcompensation using partial FWM compensation can be 20 times more efficient in terms of computational cost.

E. F. Mateo acknowledges a Postdoctoral fellowship granted by the Ministerio de Ciencia e Innovacion, Government of Spain.

References

1. E. Yamazaki, F. Inuzuka, K. Yonenaga, A. Takada, and M. Koga, "Compensation of interchannel crosstalk induced by optical fiber nonlinearity in carrier phase-locked WDM system," IEEE Photon. Technol. Lett. **19**, 9–11 (2007).
2. X. Li, X. Chen, G. Goldfarb, E. Mateo, I. Kim, F. Yaman, and G. Li, "Electronic postcompensation of WDM transmission impairments using coherent detection and digital signal processing," Opt. Express **16**, 880–888 (2008).
3. G. P. Agrawal, *Nonlinear Fiber Optics* (Academic, 2005).
4. E. Mateo, L. Zhu, and G. Li, "Impact of XPM and FWM on the digital implementation of impairment compensation for WDM transmission using backward propagation," Opt. Express **16**, 16124–16137 (2008).
5. T. Schneider, *Nonlinear Optics in Telecommunications* (Springer, 2004).